RSC Advances

PAPER

View Article Online
View Journal | View Issue

Open Access Article. Published on 25 January 2019. Downloaded on 12/4/2025 9:15:51 PM.
This article is licensed under a Creative Commons Attribution-NonCommercial 3.0 Unported Licence.

Check for updates

Cite this: *RSC Adv.*, 2019, **9**, 3486

Synthesis of novel rambutan-like graphene@aluminum composite spheres and non-destructive terahertz characterization†

Zhongbo Yang,[ab] Shuanglong Feng,*[ab] Wei Yao,[a] Jiaguang Han[c] and Huabin Wang*[ab]

Received 4th November 2018
Accepted 8th January 2019

DOI: 10.1039/c8ra09129c

rsc.li/rsc-advances

Graphene reinforced Al (graphene@Al) spheres were synthesized using microwave plasma chemical vapor deposition technique in which H_2, CH_4, and Ar were used as the reduced gas, carbon source, and plasma enhancement gas, respectively. The obtained graphene@Al spheres presented a rambutan-like structure and had a graphene shell wrapped on the sphere surface, which was proved by scanning electron microscopy, X-ray diffraction, X-ray photoelectron spectroscopy, and Raman spectroscopy. The thickness of the graphene shell on the Al sphere is difficult to be characterized by conventional techniques. However, it was successfully measured with a sophisticated terahertz (THz) time-domain spectroscopic technique. To the best of our knowledge, neither have graphene@Al spheres been synthesized before nor has a THz-based technique been exploited to characterize the thickness of a shell structure. Therefore, the present work sheds useful insights on both the rational synthesis and non-destructive characterization of graphene reinforced functional structures.

1. Introduction

Aluminum (Al) is possibly the most important metal used for metal matrix composites, due to its low costs and excellent physical properties, such as its light weight, ductility, high thermal and electrical conductivity *etc.*[1–3] In recent years, the advancement in aerospace, automotive, and shipbuilding industries has spurred the development of Al matrix composites with superior functional properties.[4–6]

Graphene is a two-dimensional carbon material formed through sp^2 bonds. The intrinsic structural character of graphene endows it with many favorable properties, *e.g.*, high interfacial affinity for metal based on its high specific surface area, excellent mechanical properties due to the sp^2 bonds, and attractive abilities in impeding atomic diffusion, which can be ascribed to its planar structure.[7,8] Consequently, graphene is regarded as a very promising reinforcing agent to improve the performance of Al-based materials by synthesizing graphene@Al composites.

Since the first graphene reinforced Al matrix composite was reported in 2011, graphene reinforced Al, Cu, Ni, Mg, Fe alloy,[9–13] and intermetallic compound matrix composites have been obtained by different processing techniques, including powder metallurgy,[14] melting and solidification,[15] thermal spray,[16] electrochemical deposition,[17] *etc.* Although great success has been achieved, it was difficult to synthesize high quality graphene reinforced composites in the previous studies because the dispersion and uniformity of graphene could not be well controlled, where procedures such as metallurgy, melting, spray and deposition were involved. Therefore, new techniques need to be developed to obtain high quality graphene-reinforced composites.

In the present study, we developed a microwave plasma chemical vapor deposition (MPCVD) approach by which graphene encapsulated Al matrix composite, namely rambutan-like graphene@Al spheres, have been synthesized in a controllable way. The rambutan-like composite is more preferred than its non-spherical counterpart in the fabrication of high-quality proximate matters as fewer defects and more even structures are likely to form inside the proximate matters made of spherical composites than the non-spherical counterparts.[18,19] This type of composite material holds great potential applications in fabrication of high-strength and tenacity Al alloy proximate matter. The morphology, composition, and structure of the as-synthesized graphene@Al spheres were verified by scanning electron microscopy, X-ray diffraction, X-ray photoelectron spectroscopy, and Raman spectroscopy. In addition, considering that the thickness of the graphene shell can influence the

[a]*Chongqing Institute of Green and Intelligent Technology, Chinese Academy of Sciences, 266 Fangzheng Avenue, Beibei District, Chongqing 400714, China. E-mail: fengshuanglong@cigit.ac.cn; wanghuabin@cigit.ac.cn*

[b]*Chongqing Engineering Research Center of High-Resolution and Three-Dimensional Dynamic Imaging Technology, 266 Fangzheng Avenue, Beibei District, Chongqing 400714, China*

[c]*Center for Terahertz Waves, College of Precision Instrument and Optoelectronics Engineering, Tianjin University, 92 Weijin Road, Nankai District, Tianjin 300072, China*

† Electronic supplementary information (ESI) available. See DOI: 10.1039/c8ra09129c

This journal is © The Royal Society of Chemistry 2019

Open Access Article. Published on 25 January 2019. Downloaded on 12/4/2025 9:15:51 PM. This article is licensed under a Creative Commons Attribution-NonCommercial 3.0 Unported Licence.

function of the composite spheres,[20–23] we also characterized the thickness of the graphene shell on the graphene@Al spheres by creatively using a self-developed non-destructive terahertz wave (THz)-based spectroscopic technique (see the ESI† for details). THz generally refers to the electromagnetic band in the frequency range from 0.1 THz to 10 THz (wavelength from 3 mm to 30 μm), and THz-based material characterization is an emerging field that has been attracting increasing attention in the material science field.[24–26] In the past years, THz-based techniques have been employed to detect the defects in functional materials and/or structures,[27] yet they have not been used to characterize sub-structures of synthesized composites. Our results show that the synthetic conditions such as the ratio of flow rates of CH_4, H_2, and Ar, and the synthesis duration can significantly influence the properties of the graphene shell on the graphene@Al spheres, in terms of morphology and thickness, and that the measured thickness of the graphene shell increases with the synthesis duration.

Compared to those previous methods of fabricating graphene reinforced composites, our MPCVD approach can be easily implemented to obtain high-quality, pure graphene-reinforced Al matrix composite, and no tedious work is required to separate the graphene@Al spheres from the product produced in the synthetic process. Besides, the THz characterization approach developed is also a new and innovative technique that can be exploited to measure the thickness of the graphene shell on the Al spheres non-destructively. To the best of our knowledge, neither the approach of synthesizing graphene@Al spheres nor the non-destructive THz-based technique for measuring the graphene shell thickness has been reported previously. Hopefully, the techniques demonstrated in this work can promote the rapid synthesis of graphene encapsulated functional particles rationally, and provide a new and convenient means to characterize shell structures on microparticles.

2. Experimental

2.1. Synthesis of rambutan-like graphene@Al spheres

Graphene@Al composite spheres were synthesized with a MPCVD setup consisting of a domestic microwave oven, a vacuum controller, a quartz tube, and a vacuum pump (see Fig. S1 in the ESI† for the schematic principle and the photograph of the setup). Al spheres (100 μm in diameter, 2A12, AMC powder Co., China) were taken as the metal base. They were firstly dried for 5–10 min in a quartz boat in the microwave, followed by loading into a quartz tube. Subsequently, the quartz tube was placed in the quartz boat and sealed together with the vacuum pump and gas tube in the microwave. High purity argon (Ar, 99.99%), hydrogen (H_2, 99.99%), and methane (CH_4, 99.99%) were used as the plasma enhancement gas, the reduced gas, and the carbon source, respectively, for the synthesis of graphene@Al composite spheres. The flow rate of the Ar gas was controlled at 100 sccm, while the other gases were adjusted according to experimental design. During the synthesis process, the temperature inside the oven was controlled by setting the power (800 W) and the running time (15 min, 30 min, or 60 min) of the microwave oven, and the temperature was measured by an infrared detector to be 450 °C. CH_4 was decomposed under the action of H_2 plasma, leading to the formation of graphene layers on the surface of the Al spheres. The reaction was terminated by powering off the microwave oven, and the synthesized composite was taken out of the quartz tube 3 min later for further tests.

2.2. Morphology and structure characterization

The morphology of the synthesized composite spheres was examined using a scanning electron microscope (FE-SEM, JSM-7800F, JEOL Ltd., Tokyo, Japan). X-ray diffraction (XRD) was used to determine the atomic structures of the as-synthesized composite spheres. XRD experiments were performed at room temperature with a diffractometer (X'Pert PRO, PANalytical B.V., Netherlands) using Cu Kα radiation. X-ray photoelectron spectroscopy (XPS) and Raman spectroscopy were used to confirm the composition and structure of the synthesized composite spheres. XPS experiments were performed with a Kratos XSAM 800 spectrometer (Kratos Analytical Ltd., Manchester, UK) equipped with a Mg Kα (1253.6 eV) X-ray source. The Raman spectrum of the composite spheres was recorded on a Bruker Vertex70 FTIR spectrometer (BrukerOptik GmbH, Ettlingen, Germany).

2.3. THz transmission spectrum measurement

The thickness of the graphene shell on the Al spheres was measured using a THz-based technique (see the ESI† for details). To prepare the samples for the THz measurement, 140 mg polyethylene (PE) powder (Sigma-Aldrich Co. Ltd., Shanghai, China) was evenly mixed with 20 mg Al spheres or the as-synthesized composite spheres (graphene@Al spheres) using an agate mortar. Subsequently, the mixture was transferred into the stainless steel mold of a hydraulic press (TianGuang Optical Instruments Co. Ltd., Tianjin, China), and a pressure of about 20 MPa was applied on the mixture for 2 min so as to obtain a disk-like sample (the experimental group) with a thickness of about 1.16 mm and a diameter of about 13.0 mm. Following the same procedure, PE powder (160 mg) was also pressed into a disk to use as the control. A terahertz time-domain spectrometer (THz-TDS, T-ray 5000, Advanced Photonix Inc., New York, NY, USA) with a dynamic range of about 76 dB and a spectral resolution of 3.13 GHz was employed in our experiments. The experiments were repeated three times, independently, with three parallel samples each time.

3. Result and discussion

As can be seen from the SEM images that the raw Al spheres are relatively smooth (Fig. 1a) and have finer grain structures on the surface (Fig. 1b). The as-synthesized composite spheres are rambutan-like (Fig. 1c) and have a shape similar to the raw Al spheres. However, the as-synthesized composite spheres present a rough and fuzzy surface (Fig. 1c and d), indicating that some new structure formed on the Al spheres. It is observed that

Open Access Article. Published on 25 January 2019. Downloaded on 12/4/2025 9:15:51 PM.
This article is licensed under a Creative Commons Attribution-NonCommercial 3.0 Unported Licence.

the newly formed fuzzy microstructures are densely compacted on the surface of the composite spheres (Fig. 1d).

In order to determine the changes on surface of the Al spheres after the synthesis, XRD, XPS, and Raman spectroscopy were employed to investigate the composition and structure of the synthesized spheres (grown for 5 min). XRD patterns of the composite spheres after MPCVD processing are presented in Fig. 2a, from which the peaks of Al(111), Al(200), Al(220), and Al(113) can be clearly observed, suggesting that the crystal of Al was still intact and nothing was doped into the Al spheres.[28] XPS was also employed to analyze the composition of the as-synthesized spheres, on consideration of the penetration ability of XPS. As shown in Fig. 2b, two peaks (73.5 eV and 75.2 eV) corresponding to Al $2p^{1/2}$ and Al $2p^{3/2}$ were identified, indicating that the base metal (Al) still maintained its original structure. In addition, the peaks for C sp^2 (284.8 eV) and C sp^3 (286.4 eV) were also observed in the XPS spectrum (Fig. 2c), in which the peak for C sp^2 is dominant. Because the presence of the C sp^2 peak indicates a carbon-based planar structure, the XPS data strongly imply that carbon-based planar structures, very likely layered graphene structures, were formed on the Al spheres' surface. To further confirm the structure of the as-synthesized spheres, they were also measured by Raman spectroscopy. As shown in Fig. 2d, a G peak (1620 cm^{-1}), a D peak (1343 cm^{-1}), a weak 2D peak (2686 cm^{-1}), and a D + G combination scattering peak (2963 cm^{-1}) were observed, and the ratio of intensity of the D peak to G peak was about 1.02 (I_D/I_G).[29] This observation corroborates that layered graphene was formed on the surface of the Al spheres. From the above characterizations, it can be concluded that the as-synthesized composite spheres mainly included two parts, *viz.* an Al sphere core and a graphene shell (formed by graphene sheets/flakes), despite that the graphene had some defects and a few graphite impurities existed in the shell.

To find the optimal condition for growing graphene microstructures on the Al spheres, we investigated the morphological evolution by changing the ratio of the flow rates between CH_4 and H_2 in the synthesis of graphene@Al spheres (Fig. 3). Fig. 3a and e indicate that the sphere surface was fully covered by non-uniform granules when the ratio of flow rates of $CH_4 : H_2 : Ar$ was set to 25 : 75 : 100. Spheres with smaller and evenly distributed granules on the spherical surface could be achieved when the flow rates' ratio of $CH_4 : H_2 : Ar$ was changed to

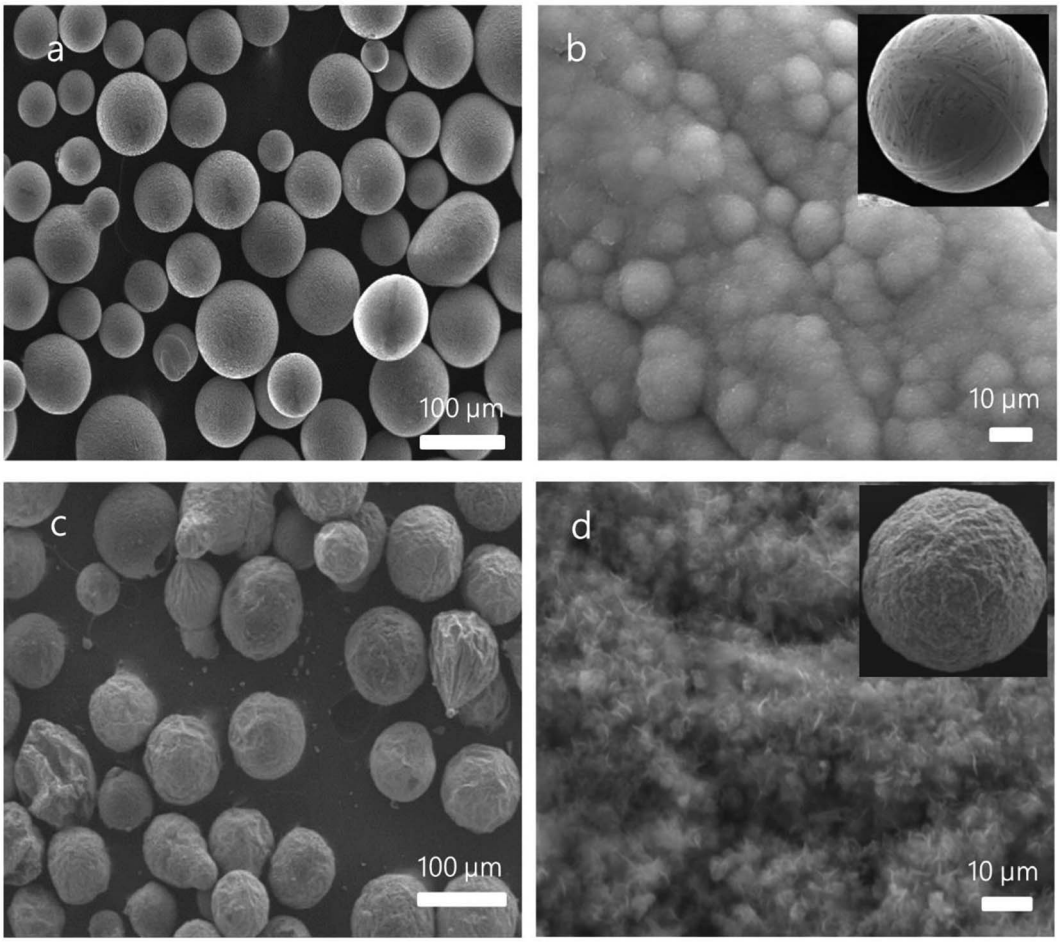

Fig. 1 SEM images of raw Al spheres and as-synthesized graphene@Al spheres. (a) SEM images of raw Al spheres; (b) a high magnification image showing the surface of a raw Al sphere (inset shows a raw Al sphere); (c) composite spheres synthesized under a $H_2 : CH_4 : Ar$ flow ratio of 15 : 85 : 100 for 30 min at 450 °C; and (d) a high magnification image showing the surface of a as-synthesized sphere (inset shows a as-synthesized sphere).

Open Access Article. Published on 25 January 2019. Downloaded on 12/4/2025 9:15:51 PM.
This article is licensed under a Creative Commons Attribution-NonCommercial 3.0 Unported Licence.

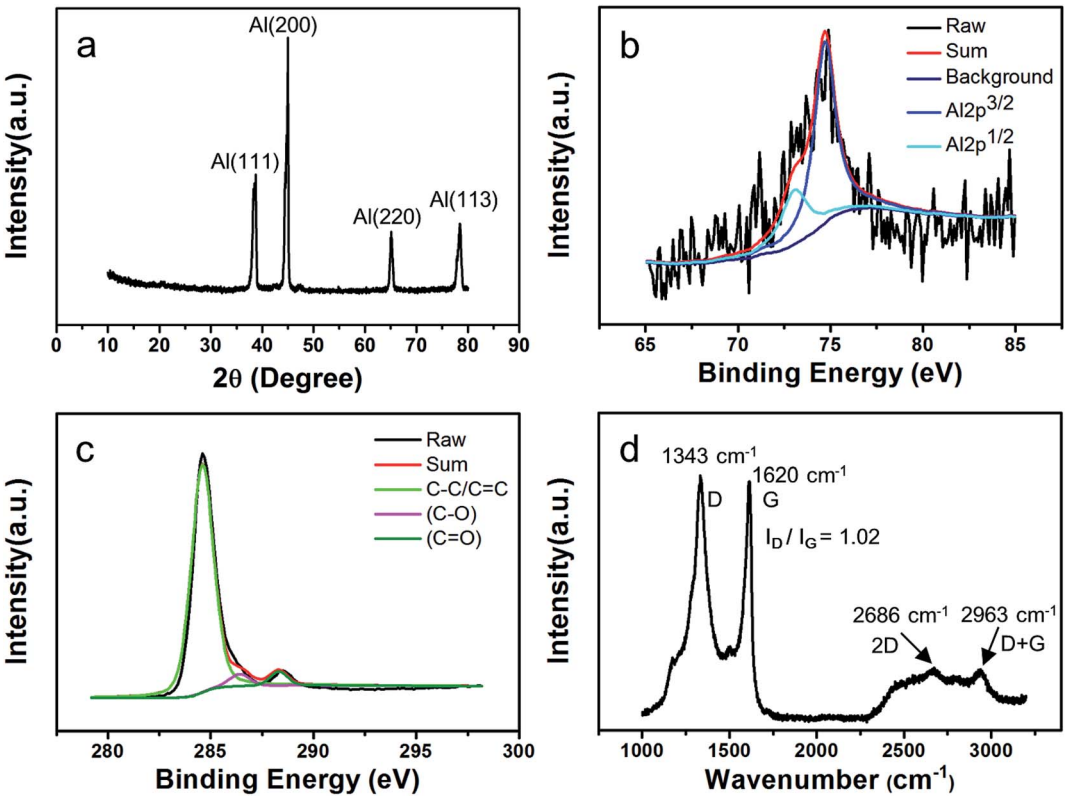

Fig. 2 The characterization of the as-synthesized composite spheres. (a) XRD pattern; (b) and (c) XPS spectra of Al 2p and C 1s, respectively; and (d) Raman spectrum.

20 : 80 : 100 (Fig. 3b and f). As the ratio of the flow rates was further reduced to 15 : 85 : 100, spheres with few granules on their surface could be synthesized (Fig. 3c and g). If the ratio of the flow rates between CH_4 : H_2 : Ar was further adjusted to 10 : 90 : 100, granules on the spherical surface could be observed again (Fig. 3d and h). Comparing the above results, we suggest that the optimal ratio of flow rates of CH_4 : H_2 : Ar was 15 : 85 : 100, in order to obtain composite spheres with a surface in good condition, *i.e.*, a surface with minimal particulate structures. The graphene@Al composite spheres with particulate structures on the surface have some obvious drawbacks, for example, they are mechanically unstable because the particulates can easily fall off the composite spheres.[19] Therefore, graphene@Al spheres with minimal particulate structures on their surface are preferred for later applications.

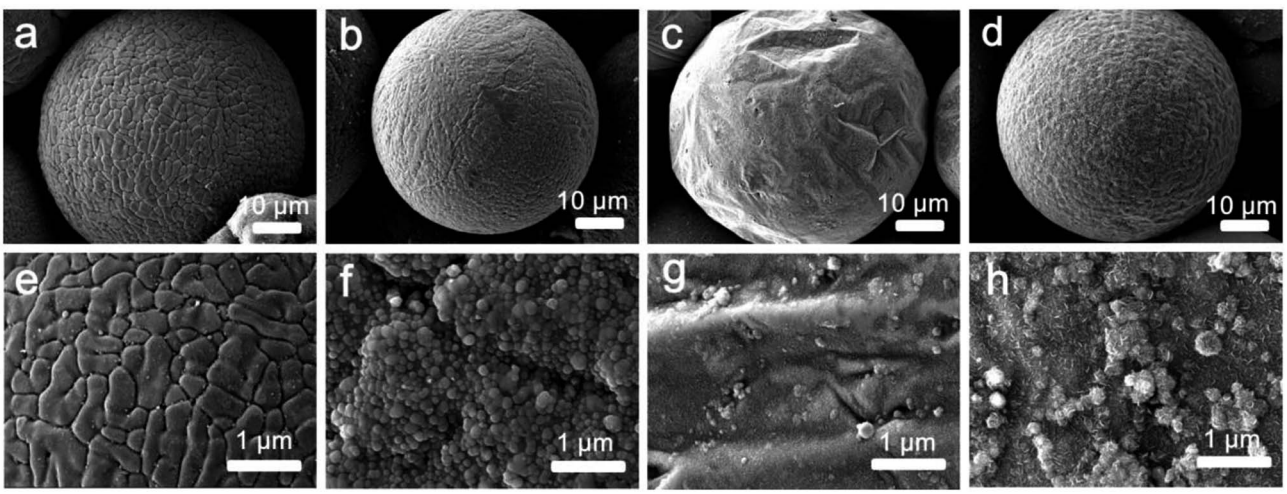

Fig. 3 SEM micrographs of the graphene@Al spheres synthesized with different CH_4 : H_2 : Ar flow ratios. 25 : 75 : 100 for (a) and (e), 20 : 80 : 100 for (b) and (f), 15 : 85 : 100 for (c) and (g), and 10 : 90 : 100 for (d) and (h). The synthesis lasted for 15 min under the above mentioned conditions. (e), (f), (g), and (h) are zoomed-in images from (a), (b), (c), and (d), respectively, to show the local features of the spheres.

Open Access Article. Published on 25 January 2019. Downloaded on 12/4/2025 9:15:51 PM.
This article is licensed under a Creative Commons Attribution-NonCommercial 3.0 Unported Licence.

Subsequently, we investigated the influence of synthesis duration on the morphology of graphene@Al spheres by extending the synthesis duration to 60 min at the optimized CH_4, H_2, and Ar flow rates, *viz.* 15 sccm, 85 sccm, and 100 sccm, respectively. Fig. 4a and b indicate that the Al sphere surface was fully covered by a shell formed by graphene sheets/flakes. However, compared to the spheres synthesized in 15 min (Fig. 3c and g) and in 30 min (Fig. 1c and d), longer synthesis duration (60 min) led to a more fuzzy composite sphere surface, possibly due to more graphene sheets getting encapsulated on the Al sphere surface. The above evidence suggests that the structure of graphene shell on the Al spheres can be regulated by adjusting the synthesis duration.

The evaluation of the thickness of the graphene shell on the Al spheres is an essential study because it affects the properties as well as the performance of the graphene@Al spheres. In the traditional way, this can be done by carrying out SEM/TEM experiments to collect graphs of graphene@Al spheres, from which average diameter of the particles can be calculated statistically. Afterwards, the thickness of graphene shell can be derived from the comparison of the diameters of the Al spheres and graphene@Al spheres. However, some drawbacks in this approach can influence the reliability of the calculated results. In SEM/TEM measurement, the electronic beam is focused on a certain plane of the sample, and then micrographs are collected for the sample. Because the particles out of the focus plane cannot be accurately characterized, the obtained diameter of the particles from the micrographs can deviate from the true size of the particles. Moreover, it is common that the particles in the samples for SEM/TEM measurement overlap with each other, which makes measuring the size of individual particles from the collected SEM/TEM micrographs difficult. Therefore, a new technique is required to measure the diameter of the graphene@Al spheres, from which the thickness of graphene shell on the Al spheres can be ascertained.

In the present study, a THz-TDS technique was employed to measure the average diameters of the graphene@Al spheres with different synthesis durations. The setup for the experiment is given in Fig. 5.

In this technique, the time domain electric field signal ($E(t)$) was measured for the experimental and control samples,

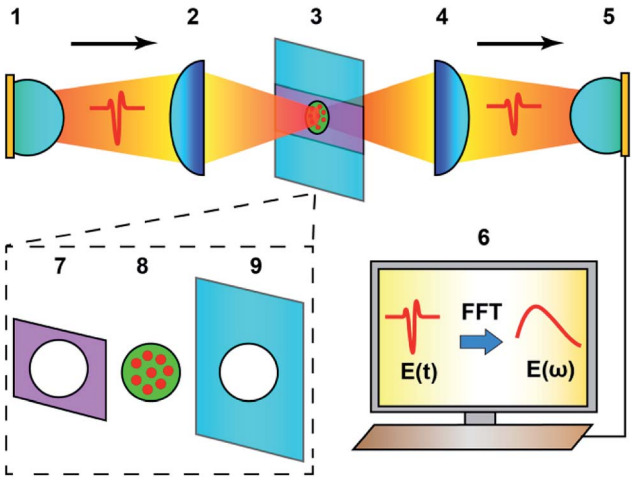

Fig. 5 Schematic of the THz-TDS measurement system. THz wave emitted from (1) an THz emitter was focused by (2) a high-density polyethylene (HDPE) plano-convex lens onto a disk-like sample (red dots distributed in a green matrix) which was fixed in (3) a sample holder. The THz wave transmitted through the sample was then collected by (4) another HDPE plano-convex lens and detected by (5) a THz receiver. The detected signal was sent to (6) a computer for further analysis to extract the information about the sample properties. To fix the sample, (8) the sample was sandwiched between (7) an aperture magnetic plate and (9) an aperture metal plate. Al spheres or graphene@Al spheres (red dots) were embedded in the PE (the green matrix) and pressed into a disk.

respectively. Subsequently, $E(t)$ was transformed into the frequency field domain signal ($E(\omega)$) using the FFT algorithm. The transmission spectrum ($T(\omega)$) of the samples was calculated using the following formula:[30]

$$T(\omega) = I_{\mathrm{sam}}(\omega)/I_{\mathrm{ref}}(\omega) = [|E_{\mathrm{sam}}(\omega)|/|E_{\mathrm{ref}}(\omega)|]^2 \quad (1)$$

where, ω is the angular frequency of the terahertz wave; $E_{\mathrm{sam}}(\omega)$ and $E_{\mathrm{ref}}(\omega)$ are the measured electric frequency field domain signal of the experimental and control samples, respectively; $I_{\mathrm{sam}}(\omega) = |E_{\mathrm{sam}}(\omega)|^2$ and $I_{\mathrm{ref}}(\omega) = |E_{\mathrm{ref}}(\omega)|^2$ are the THz electric intensity of the experimental and control samples, respectively.

Interestingly, it was found that the transmission value (T) of the samples (Fig. 6a) can be regarded as frequency-independent for the values between 1.6 THz and 2.2 THz

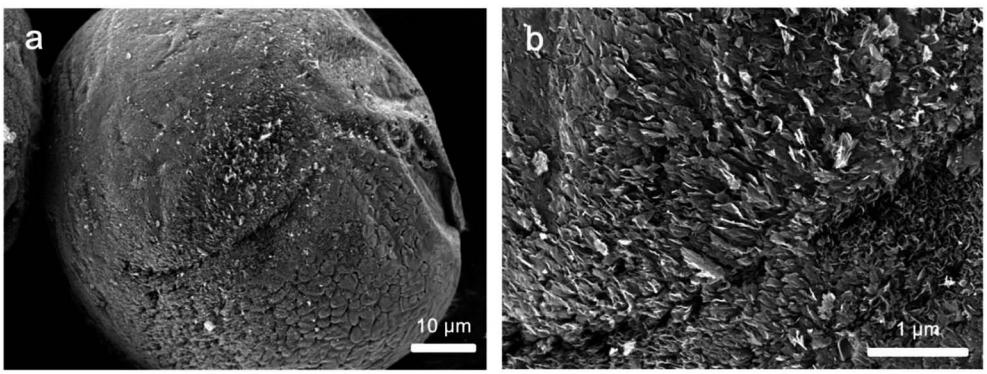

Fig. 4 SEM micrographs of a typical graphene@Al sphere with a synthesis duration of 60 min under a CH_4 : H_2 : Ar flow rate ratio of 15 : 85 : 100. (b) is a zoomed-in images from (a) to show the local features of the sphere.

Open Access Article. Published on 25 January 2019. Downloaded on 12/4/2025 9:15:51 PM.
This article is licensed under a Creative Commons Attribution-NonCommercial 3.0 Unported Licence.

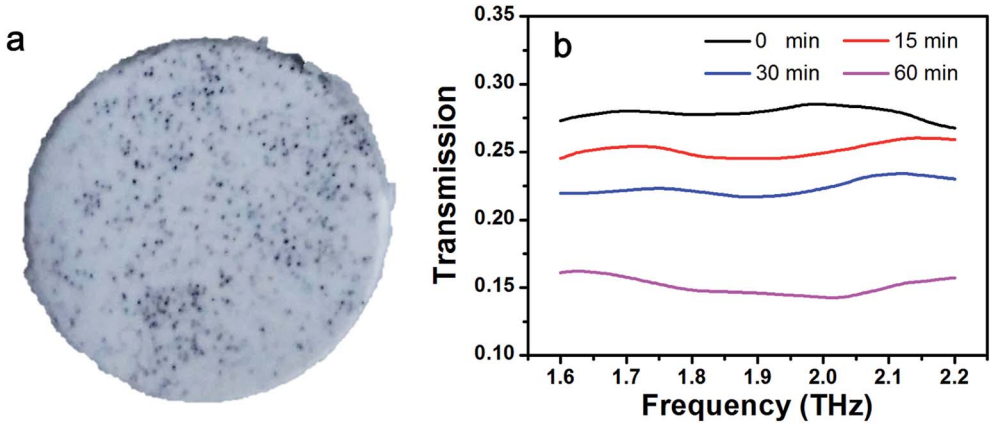

Fig. 6 The THz transmission measurement. (a) A disk-like sample prepared for the THz measurement. In the sample, microspheres (black dots are graphene@Al spheres in this case) were embedded in PE (white matrix). (b) Transmission spectra for samples of graphene@Al spheres with different synthesis durations (15 min, 30 min, and 60 min) and Al spheres (0 min).

(Fig. 6b). This was also supported by numerical calculations of the PE buried-Al spheres sample or graphene@Al spheres sample, based on the light scattering method according to the Mie theory and FDTD simulation (see the eqn (S14) and (S15) in the ESI†). $T_{0\ \mathrm{min}}$, $T_{15\ \mathrm{min}}$, $T_{30\ \mathrm{min}}$, and $T_{60\ \mathrm{min}}$ are used to denote the average transmission values in the region of 1.6 THz to 2.2 THz for the Al sphere sample, and graphene@Al sphere samples with different synthesis durations (15 min, 30 min, and 60 min). In this example, $T_{0\ \mathrm{min}}$, $T_{15\ \mathrm{min}}$, $T_{30\ \mathrm{min}}$, and $T_{60\ \mathrm{min}}$ are 0.279, 0.251, 0.224, and 0.151, respectively.

According to the theoretical calculations (see eqn (S17) in the ESI†), the THz transmission of the graphene@Al sphere samples can be calculated by

$$T = I_{\mathrm{t,\ sample}}/I_0 = \exp(-b_{\mathrm{cf}}D_{\mathrm{t}}^2), \tag{2}$$

where, I_0 is the electric field intensity of the incident THz wave, $I_{\mathrm{t,\ sample}}$ is the measured electric field intensity of the sample, b_{cf} is the corrected decay factor with a value of $5.11 \times 10^4\ \mathrm{cm}^{-2}$, and D_{t} is the average diameter of the graphene@Al spheres with different synthesis durations.

By the substitution of $T_{15\ \mathrm{min}}$, $T_{30\ \mathrm{min}}$, and $T_{60\ \mathrm{min}}$ into eqn (2), it is very convenient to obtain the diameters of the graphene@Al spheres, which were found to be 104.06 μm, 108.26 μm, and 121.7 μm, respectively. The corresponding average thickness of the graphene shell on the Al spheres were 2.03 μm, 4.13 μm, and 10.85 μm by assuming that the average diameter of the Al spheres is 100 μm. The values are comparable to the derived thickness of graphene shells, *viz.* 2.21 μm, 4.22 μm, and 10.77 μm, of the corresponding graphene@Al spheres measured (nearly 100 spheres for each group of samples) from SEM micrographs.

4. Conclusion

In summary, rambutan-like graphene shell wrapped Al spheres, namely graphene@Al spheres were synthesized using an MPCVD approach. The structure of the composite spheres was characterized by SEM, XRD, XPS, and Raman spectroscopy. The experimental conditions for achieving high-quality graphene@Al spheres were also investigated. The advantages of this synthetic strategy lie in its low-cost, simplicity, mild reaction conditions, and the capability to control the morphology of the graphene covered Al microstructures by programming the experimental parameters. More importantly, the thickness of the graphene shell on the graphene@Al spheres was successfully examined using a unique non-destructive THz-TDS technique. The present work provides new insights on synthesizing graphene@Al composites in a cost-effective and high-yield fashion, and a new means to measure the size of the microspheres, which is not readily possible by other spectroscopic or imaging techniques. The techniques demonstrated in this work can undoubtedly find application in the synthesis of functional spheres and characterization of the properties of microstructures.

Conflicts of interest

The authors declare no conflict of interest.

Acknowledgements

This work was financially supported by the National Key Research and Development Program of China (2017YFF0106303, 2016YFC0101002, 2016YFC0101301), Central Government Supported Key Instrument Program of China (YXGYQ201700136), National Natural Science Foundation of China (61605207, 11604332), the Chongqing Science and Technology Commission (Y500061LH1), and the Chinese Academy of Sciences for a Key Scientific Instrument and Equipment Development Project.

References

1 W. S. Miller, L. Zhuang, J. Bottema, A. J. Witterbrood, P. De Smet, A. Haszler and A. Vieregge, *Mater. Sci. Eng., A*, 2000, **280**, 37–49.

Open Access Article. Published on 25 January 2019. Downloaded on 12/4/2025 9:15:51 PM.
This article is licensed under a Creative Commons Attribution-NonCommercial 3.0 Unported Licence.

2 C. Genevois, D. Fabregue, A. Deschamps and W. J. Poole, *Mater. Sci. Eng., A*, 2006, **441**, 39–48.
3 H. A. Ellis, J. H. McCarthy and J. Herrington, *J. Clin. Pathol.*, 1979, **32**, 832–844.
4 J. Singh and A. Chauhan, *Ceram. Int.*, 2016, **42**, 56–81.
5 N. T. Aboulkhair, I. Maskery, C. Tuck, I. Ashcroft and N. M. Everitt, *Mater. Des.*, 2016, **104**, 174–182.
6 P. S. Reddy, R. Kesavan and B. V. Ramnath, *Silicon*, 2018, **10**, 495–502.
7 A. K. Geim, *Science*, 2009, **324**, 1530–1534.
8 C. Lee, X. D. Wei, J. W. Kysar and J. Hone, *Science*, 2008, **321**, 385–388.
9 J. H. Liu, U. Khan, J. Coleman, B. Fernandez, P. Rodriguez, S. Naher and D. Brabazon, *Mater. Des.*, 2016, **94**, 87–94.
10 N. VijayPonraj, A. Azhagurajan, S. C. Vettivel, X. Sahaya Shajan, P. Y. Nabhiraj and M. Sivapragash, *Surf. Interfaces*, 2017, **6**, 190–196.
11 J. Wozniak, P. Kurtycz, K. Broniszewski, M. Kostecki, J. Morgiel and A. Olszyna, *Mater. Today Proc.*, 2015, **2**, 376–382.
12 M. Rashad, F. S. Pan and M. Asif, *Graphene materials: fundamentals and emerging applications*, ed. A. Tiwari and M. Syvajarvi, Hoboken, New Jersey, USA 2015, pp. 153–189.
13 L. Wang, J. F. Jin, J. G. Cao, P. J. Yang and Q. Peng, *Crystals*, 2018, **8**, 160.
14 H. Kwon, J. Mondal, K. A. Alogab, V. Sammelselg, M. Takamichi, A. Kawaskiet and M. Leparoux, *J. Alloys Compd.*, 2017, **698**, 807–813.
15 A. E. Karantzalis, A. Lekatou and K. Tsirka, *Mater. Charact.*, 2012, **69**, 97–107.
16 K. Kang, G. Bae, B. Kim and C. Lee, *Mater. Chem. Phys.*, 2012, **133**, 495–499.
17 K. Jagannadham, *Metall. Mater. Trans. B*, 2012, **43**, 316–324.
18 D. Z. Wang, C. F. Yu, X. Zhou, J. Ma, W. Liu and Z. J. Shen, *Appl. Sci.*, 2017, **7**, 430.
19 E. O. Olakanmi, R. F. Cochrane and K. W. Dalgarno, *Prog. Mater. Sci.*, 2015, **74**, 401–477.
20 C. Sun, *Plasmonics*, 2018, **13**, 1671–1680.
21 S. Bhardwaj, R. Uma and R. P. Sharma, *Plasmonics*, 2017, **12**, 961–969.
22 M. J. Wan, Y. Li, J. W. Chen, W. Y. Wu, Z. Chen, Z. L. Wang and H. T. Wang, *Sci. Rep.*, 2017, **7**, 32.
23 S. L. Ye, H. H. Huang, C. L. Yuan, F. Liu, M. Zhai, X. Z. Shi, C. Qi and G. F. Wang, *J. Nanomater.*, 2014, 989672.
24 C. Lee, J. Y. Kim, S. Bae, K. S. Kim, B. H. Hong and E. J. Choi, *Appl. Phys. Lett.*, 2011, **98**, 071905.
25 L. Ju, B. S. Geng, J. Horng, C. Girit, M. Martin, Z. Hao, H. A. Bechtel, X. G. Liang, A. Zettl, Y. R. Shen and F. Wang, *Nat. Nanotechnol.*, 2011, **6**, 630–634.
26 B. Sensale-Rodriguez, T. Fang, R. S. Yan, M. M. Kelly, D. Jena, L. Liu and H. L. Xing, *Appl. Phys. Lett.*, 2011, **99**, 113104.
27 J. D. Buron, D. H. Petersen, P. Boggild, D. G. Cooke, M. Hilke, J. Sun, E. Whiteway, P. F. Nielsen, O. Hansen, A. Yurgens and P. U. Jepsen, *Nano Lett.*, 2012, **12**, 5074–5081.
28 Z. Y. Cui, X. G. Li, H. Zhang, K. Xiao, C. F. Dong, Z. Y. Liu and L. W. Wang, *Adv. Mater. Sci. Eng.*, 2015, 163205.
29 A. C. Ferrari, J. C. Meyer, V. Scardaci, C. Casiraghi, M. Lazzeri, F. Mauri, S. Piscanec, D. Jiang, K. S. Novoselow, S. Roth and A. K. Geim, *Phys. Rev. Lett.*, 2006, **97**, 187401.
30 Y. Y. Wang, T. Notake, M. Tang, K. Nawata, H. Ito and H. Minamide, *Phys. Med. Biol.*, 2011, **56**, 4517–4527.

 This journal is © The Royal Society of Chemistry 2019